

Bulky 4-phosphacyclohexanones: diastereoselective complexations, orthometallations and unprecedented [3.1.1]metallabicycles

Ruth Doherty, Mairi F. Haddow, Zoë A. Harrison, A. Guy Orpen,* Paul G. Pringle,* Alex Turner and Richard L. Wingad

Received 26th May 2006, Accepted 27th June 2006

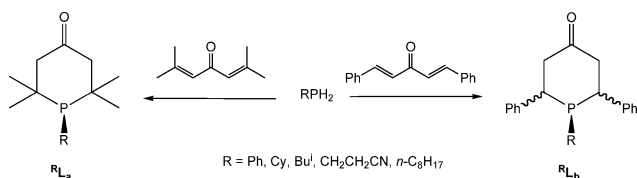
First published as an Advance Article on the web 26th July 2006

DOI: 10.1039/b607490a

The 4-phosphacyclohexanones, 2,2,6,6-tetramethyl-1-phenyl-4-phosphorinanone (L_a), 1,2,6-triphenyl-4-phosphorinanone ($^{Ph}L_b$), 1-cyclohexyl-2,6-diphenyl-4-phosphorinanone ($^{Cy}L_b$) and 1-*tert*-butyl-2,6-diphenyl-4-phosphorinanone ($^{Bu}L_b$) have been made by modifications of literature methods. Phosphines $^R L_b$ are each formed as mixtures of *meso*- and *rac*-diastereoisomers. Isomerically pure *rac*- $^{Ph}L_b$, *rac*- $^{Cy}L_b$ and *meso*- $^{Bu}L_b$ can be isolated by recrystallisation from MeCN. Heating mixtures of isomers of $^R L_b$ with TsOH leads to isomerisations to give predominantly the *meso*- $^R L_b$. The complex *trans*-[PdCl₂(L_a)₂] (**1**) is readily made from [PdCl₂(NCPH₂)] but the analogous platinum complex **2** has not been detected and instead, cyclometallation at the 3-position (α to the ketone) in the phosphacycle occurs to give *trans*-[PtCl(L_a)(L_a -3H)] (**3**) (where L_a -3H = L_a deprotonated at the 3-position) featuring a [3.1.1]metallabicyclic structure as confirmed by X-ray crystallography. The analogous palladabicyclic **4** has been detected upon treatment of **1** with Et₃N in refluxing toluene. The type of complex formed by $^R L_b$ depends on which diastereoisomer (*meso* or *rac*) is involved. *rac*- $^{Ph}L_b$ (a mixture of *R,R*- and *S,S*-enantiomers, labelled α and β) forms *trans*-[MCl₂(*rac*- $^{Ph}L_b$)₂], M = Pd (**5**) or Pt (**6**), as mixtures of diastereoisomers ($\alpha\alpha/\beta\beta$ and $\alpha\beta$ forms). The structure of $\alpha\alpha$ -**6** has been determined by X-ray crystallography. Ligand competition experiments monitored by ³¹P NMR showed that Pd(II) and Pt(II) have a significant preference to bind *rac*- $^{Ph}L_b$ over *meso*- $^{Ph}L_b$. *meso*- $^{Bu}L_b$ reacts with [PtCl₂(NCBu^t)₂] under ambient conditions to give the binuclear complex [Pt₂Cl₂(*meso*- $^{Bu}L_b$ -2'H)₂] (**7**) where orthometallation has occurred on one of the exocyclic phenyl substituents as confirmed by X-ray crystallography. *rac*- $^{Bu}L_b$ reacts with [PtCl₂(NCBu^t)₂] to give a mononuclear cyclometallated species assigned the structure *trans*-[PtCl(*rac*- $^{Bu}L_b$ -2'H)($^{Bu}L_b$)] (**8**) on the basis of its ³¹P NMR spectrum. *rac*- $^{Cy}L_b$ reacts with [PtCl₂(NCBu^t)₂] in refluxing toluene to give *trans*-[PtCl₂(*rac*- $^{Cy}L_b$)₂] (**9**) and the crystal structure of $\alpha\beta$ -**9** has been determined.

Introduction

The reaction of primary phosphines with dienones to give bulky 4-phosphacyclohexanones (4-phosphorinanones) was first reported¹ by Welcher and Day in 1962 (Scheme 1).



Scheme 1

To date, the work reported on 4-phosphorinanones has primarily concerned ring conformational analysis^{2,3} and their coordination chemistry remains unexplored.

4-Phosphorinanones are of interest as bulky ligands for several reasons. The six-membered ring constrains the 2,6-substituents to be in close proximity to the metal which may lead to unusual

coordination chemistry and catalytic activity; indeed bulky 4-phosphorinanones have been claimed as ligands for Pd-catalysed alkene carbonylation⁴ and, while this work was in progress, the application of related phosphorinanones in Pd-catalysed C–C coupling reactions has been reported.⁵ There is the potential to vary the 2,6-substituents on the ring enabling manipulation of the ligand stereoelectronic effects. Finally, the carbonyl group should allow further elaboration of the ligand at a site remote from the donor atom.

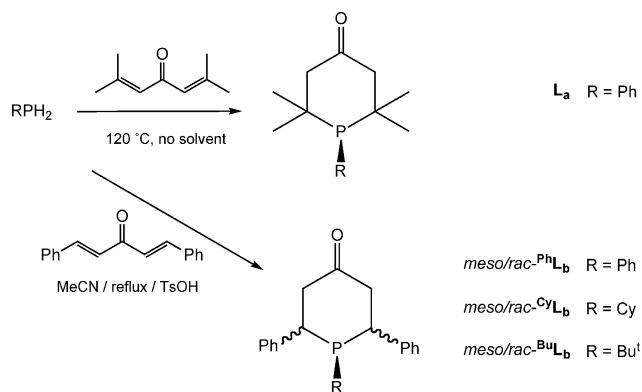
In this paper the coordination chemistry of the 4-phosphorinanones shown in Scheme 2 with palladium(II) and platinum(II) is reported including the observation of cyclometallation at different sites on the ligand and a clear ligand diastereomeric preference in complexation.

Results and discussion

Ligand synthesis

The ligands L_a and $^R L_b$ (R = Ph, Cy and Bu^t) were made by modifications of the literature routes¹ as shown in Scheme 2 and the products were fully characterised (see Experimental section). In our hands, the solventless reaction of PhPH₂ with

School of Chemistry, University of Bristol, Bristol, UK BS8 1TS. E-mail: paul.pringle@bristol.ac.uk; Fax: +44 (0)117 925 1295; Tel: +44 (0)117 928 7645



Scheme 2

dibenzylideneacetone (*i.e.* the literature route¹ to $^{\text{Ph}}\text{L}_b$) gave several unidentified products in addition to $^{\text{Ph}}\text{L}_b$ but, by employing MeCN as solvent and an acid catalyst, only isomers of $^{\text{Ph}}\text{L}_b$ were observed.

Crystals of ligand L_a were obtained from diethyl ether. From previous conformational analysis work on six-membered phosphacycles,^{2,6} an axial Ph–P was expected in L_a and the structure of L_a in the solid state (see Fig. 1 and Table 1) confirms this assignment.

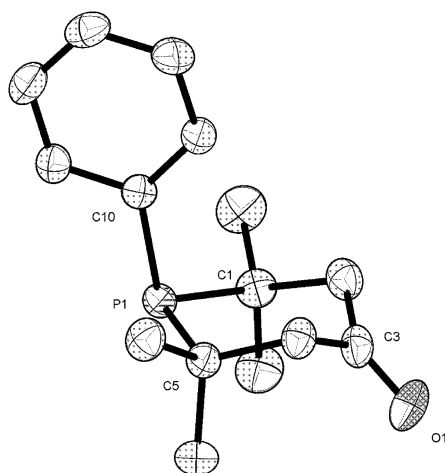
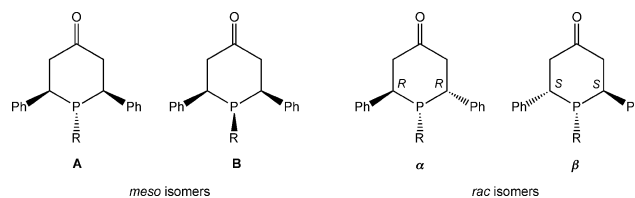


Fig. 1 Crystal structure of L_a (50% thermal ellipsoids). Hydrogen atoms removed for clarity.

Table 1 Selected bond distances (Å) and angles (°) for L_a

P1–C10	1.8359(15)	C10–P1–C5	103.23(6)
P1–C5	1.8880(14)	C10–P1–C1	104.88(6)
P1–C1	1.8875(14)	C5–P1–C1	104.19(6)

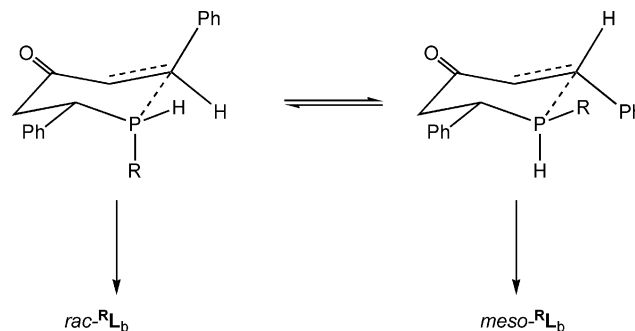
The reaction of RPH_2 ($\text{R} = \text{Ph}, \text{Cy}$ and Bu^t) with dibenzylideneacetone gave two products in each case, as evidenced by the two singlets observed in their ^{31}P NMR spectra. Theoretically, the three diastereoisomers shown in Scheme 3 are possible for $^{\text{R}}\text{L}_b$: two *meso* isomers (A and B) and a *rac* isomer (a mixture of α - and β -enantiomers). However, steric hindrance would militate against the formation of *meso*-B, with the bulky adjacent substituents *cis* to one another and therefore the two observed products are most likely to be the *meso*-A and *rac* diastereoisomers.



Scheme 3

The ratio of diastereoisomers of $^{\text{R}}\text{L}_b$ formed depends on R and the conditions used. When the syntheses were carried out in MeCN in the presence of TsOH catalyst, the approximate *meso* : *rac* ratios were 1 : 3 for $^{\text{Ph}}\text{L}_b$, 4 : 1 for $^{\text{Cy}}\text{L}_b$, and >100 : 1 for $^{\text{Bu}^t}\text{L}_b$. These data appear to correlate with the bulk of the R substituent but when the syntheses were carried out solventless and in the absence of catalyst, the ratios were 1 : 7 for $^{\text{Ph}}\text{L}_b$, 1 : 4 for $^{\text{Cy}}\text{L}_b$, and 1 : 1 for $^{\text{Bu}^t}\text{L}_b$.

Further insight into the relative stabilities of *meso*- and *rac*- $^{\text{R}}\text{L}_b$ was obtained from the observation that, when mixtures of diastereoisomers were refluxed in MeCN in the presence of TsOH catalyst, the proportion of *meso*- and *rac*-isomers changed over a period of days in favour of the *meso*- $^{\text{R}}\text{L}_b$, *e.g.* an initially 1 : 7 mixture of *meso* : *rac*- $^{\text{Ph}}\text{L}_b$ became a 3 : 1 mixture after 7 days. The *rac*- $^{\text{R}}\text{L}_b$ to *meso*- $^{\text{R}}\text{L}_b$ isomerisations show that the Michael addition is reversible and that *meso*- $^{\text{R}}\text{L}_b$ is the thermodynamically more stable isomer. It also suggests that *rac*- $^{\text{R}}\text{L}_b$ only forms when the reaction is under kinetic control. The stereochemical outcome of the reaction is determined at the cyclisation step (see Scheme 4). Assuming the pseudo-chair conformations for the transition states⁷ shown in Scheme 4, it can be understood why the initial proportions of *meso* and *rac* isomers differ from the thermodynamic ratios.



Scheme 4

The compound *rac*- $^{\text{Cy}}\text{L}_b$ was air-sensitive and crystals of its oxide suitable for X-ray crystallography were obtained from hot acetonitrile; the crystal structure (see Fig. 2 and Table 2) reveals a twist-boat conformation of the phosphorinane as occupation of pseudo-axial sites by bulky substituents (which would be inevitable in a chair conformation) is avoided.

Crystals of *meso*- $^{\text{Bu}^t}\text{L}_b$ were grown from acetonitrile solution and its structure in the solid state determined by single crystal X-ray methods. The phosphacycle adopts a near-perfect mirror symmetrical chair conformation with the phenyl and Bu^t substituents in pseudo-equatorial sites (see Fig. 3, Table 3).

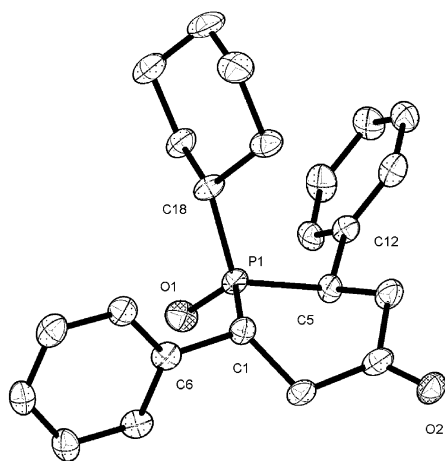


Fig. 2 Crystal structure of the oxide of *rac*- CyL_b (50% thermal ellipsoids). Hydrogen atoms removed for clarity.

Table 2 Selected bond distances (Å) and angles (°) for the oxide of *rac*- CyL_b

P1–O1	1.485(5)	O1–P1–C1	113.5(2)
P1–C18	1.817(5)	C18–P1–C1	104.6(2)
P1–C5	1.830(4)	C5–P1–C1	101.3(2)
P1–C1	1.842(5)		

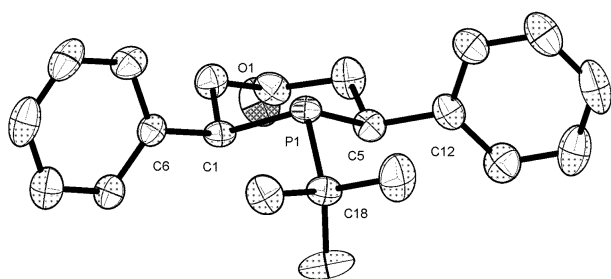


Fig. 3 Crystal structure of *meso*- BuL_b (50% thermal ellipsoids). Hydrogen atoms removed for clarity.

Table 3 Selected bond distances (Å) and angles (°) for *meso*- BuL_b

P1–C5	1.883(3)	C5–P1–C1	96.14(13)
P1–C1	1.884(3)	C5–P1–C18	102.86(13)
P1–C18	1.889(3)	C1–P1–C18	104.82(13)

From the structures of *meso*- BuL_b and the oxide of *rac*- CyL_b , it would appear that the 2,6-phenyl substituents in phosphacycles R^bL_b promote a chair conformation in the *meso*-**A** isomers and a twist conformation in the *rac* isomers, although the reported² crystal structure of the sulfide of *rac*- PhL_b has a chair conformation, with equatorial Ph–P and one axial Ph–C.

Conformational analysis of PhL_b

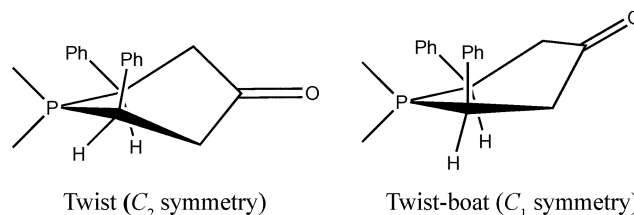
In order to probe the conformational properties of these ligands, DFT calculations were carried out on the chair and twist conformers of the *rac*, *meso*-**A** and *meso*-**B** isomers of PhL_b as shown in Scheme 5 (with Ph–P in either equatorial or axial positions). It was immediately clear that the energies of the chair conformer with P–Ph axial (ax-chair) for *meso*-**A** and the eq-chair conformer for *meso*-**B** are very high (see Table 4). This is understandable because

Table 4 Relative energies of isomers and conformers of PhL_b , calculated by DFT

Isomer	Conformation	Relative $E/\text{kJ mol}^{-1}$
<i>meso</i> - A	eq-chair	0.0
	ax-chair	40.5
	twist	30.1
<i>meso</i> - B	eq-chair	38.5
	ax-chair	23.5
	twist	16.9
<i>rac</i>	eq-chair	11.1
	ax-chair	13.2
	twist	16.9

they each contain 2,6-diaxial Ph substituents; these conformers were therefore not considered further.

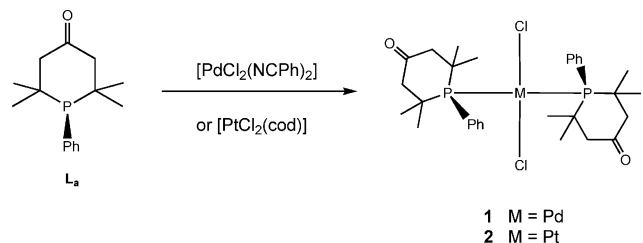
From the data in Table 4 we note the following: (1) The stability of the most energetically favoured conformers is in the sequence *meso*-**A** > *rac* > *meso*-**B**, supporting the assignment of the two isomers observed as *meso*-**A** and *rac*. (2) The conformational preferences are: (i) for the *meso*-**A** isomer, the eq-chair conformer, in which all phenyls are equatorial, has the lowest energy; (ii) for the *rac* isomer, the eq-chair, ax-chair and twist conformers are of similar energies; (iii) for the *meso*-**B** isomer, the twist conformer has the lowest energy, although the optimised geometry is better described as a twist-boat because the PC_5 ring is distorted from C_2 symmetry (see below).



Finally we note that these computed energies are enthalpies (not free energies) for isolated molecules rather than the solvated species observed in the NMR experiments, and so can only be a guide to the equilibrium behaviour of these species.

Palladium(II) and platinum(II) complexes of L_a

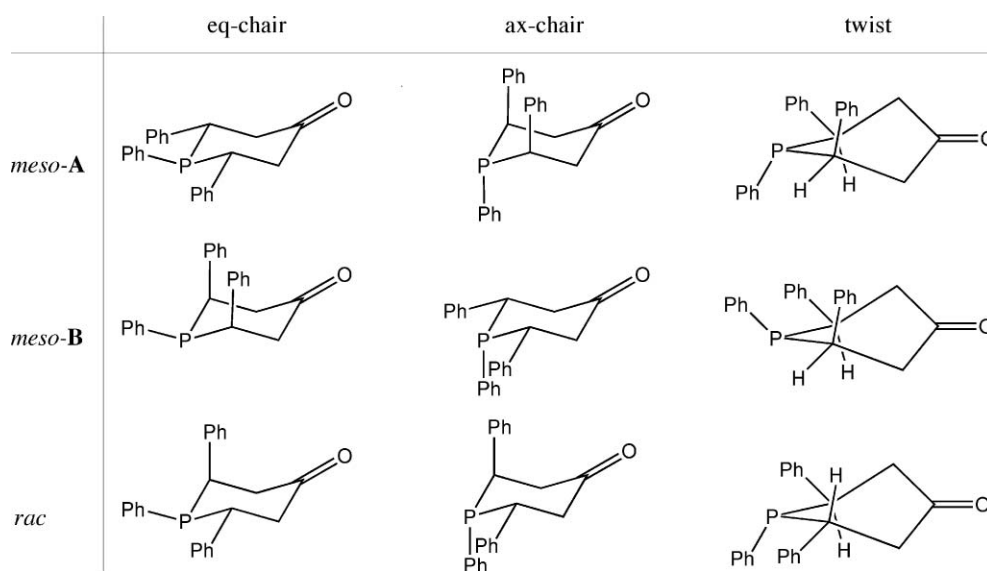
The reaction of $[\text{PdCl}_2(\text{NCPH}_2)_2]$ with 2 equivalents of L_a in toluene at room temperature resulted in the formation of the yellow *trans*- $[\text{PdCl}_2(\text{L}_a)_2]$ (**1**), which has been fully characterised (see Experimental section). The IR spectrum of **1** had a $\nu(\text{CO})$ band at 1706 cm^{-1} which is similar to the $\nu(\text{CO})$ of 1701 cm^{-1} in L_a itself.



1 M = Pd
2 M = Pt

(1)

Crystals of **1** were grown by slow evaporation of a CDCl_3 solution and the X-ray crystal structure determined. The structure of *trans*- $[\text{PdCl}_2(\text{L}_a)_2]$ (**1**) in the crystal has exact inversion symmetry



Scheme 5

Table 5 Selected bond distances (Å) and angles (°) for complex 1

Pd1–Cl1	2.3060(6)	P1–C5	1.893(2)
Pd1–P1	2.3751(6)	C10–P1–C1	101.76(10)
P1–C10	1.831(2)	C10–P1–C5	112.27(10)
P1–C1	1.882(2)	C1–P1–C5	104.69(10)

(see Fig. 4 and Table 5) with the palladium(II) centre having the expected *trans* square planar configuration. The ligands show a twist conformation with the PC₅ rings having approximate C₂ symmetry. The metal and phenyl groups therefore are in approximately isoclinal sites. The ligand orientation is such that one methyl group attached to C1 (C6, see Fig. 4) is above the metal coordination plane resulting in a pair of short Pd...H contacts (2.72 Å).

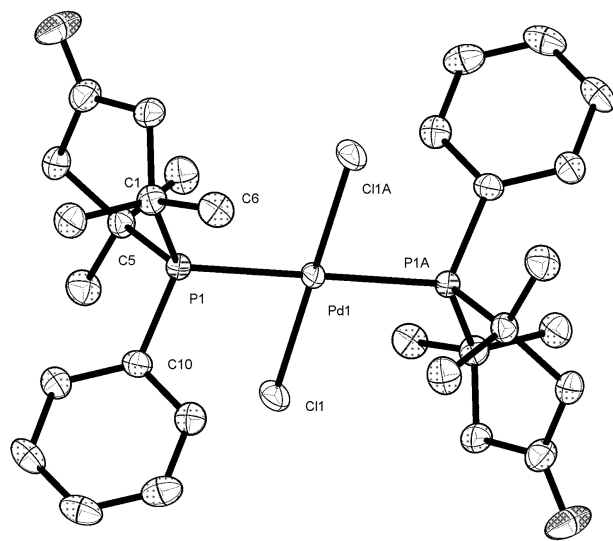
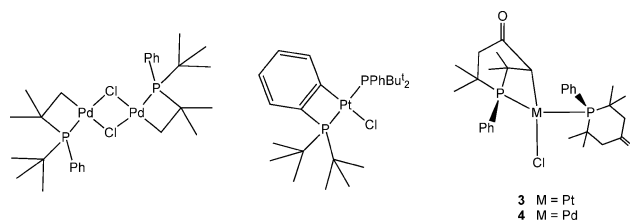


Fig. 4 Crystal structure of complex 1 (50% thermal ellipsoids). All hydrogens have been omitted for clarity. The symmetry operation invoked for the atoms with 'A' letters is (2 - x, -y, 1 - z).

When **L_a** was reacted with [PtCl₂(cod)] in a 2 : 1 ratio in dichloromethane at room temperature, the expected product was *trans*-[PtCl₂(**L_a**)₂] (**2**) but it was clear from the ³¹P NMR spectrum that **2** had not been formed. The spectrum showed an AX pattern with δ_A 38.2 ppm, ¹J(PtP_A) 2948 Hz and δ_X -13.0 ppm, ¹J(PtP_X) 2225 Hz and J(P_AP_X) 407 Hz consistent with the formation of a *trans* complex in which cyclometallation has occurred on one of the coordinated phosphines. The data for the highly shielded P_X are consistent with it being in a 4-membered ring.⁹ The ligand PhPBu₂ (an acyclic analogue of **L_a**) forms the complexes [MCl₂(PhPBu₂)₂] (M = Pd or Pt) which undergo cyclometallation on the methyl group of the *t*-butyl substituent⁹ or on the P-phenyl group¹⁰ to give the 4-membered metallacycles shown in Scheme 6. Therefore it was considered likely that the cycloplatination of **L_a** had occurred either at one of the exocyclic methyl groups or at an *ortho* position of the P-phenyl group but the crystal structure showed otherwise: metallation had taken place at the activated 3-position (the carbon α to the ketone) to give **3**.



Scheme 6

Crystals of **3** were grown by slow evaporation of its CDCl₃ solution and the X-ray crystal structure determined (see Fig. 5, Table 6). The crystal structure shows that **3** contains a [3.1.1]metallaphosphabicyclic. The platinum atom is in a distorted square planar environment, since the 4-membered ring constrains the P(2)–Pt(1)–C(17) angle to 66°. The metallated carbon C(17) is *trans* to Cl(1) and the two phosphorus atoms are *trans* to each other (P(1)–Pt(1)–P(2) 163.23(3)°). The phosphacyclohexane ligand at

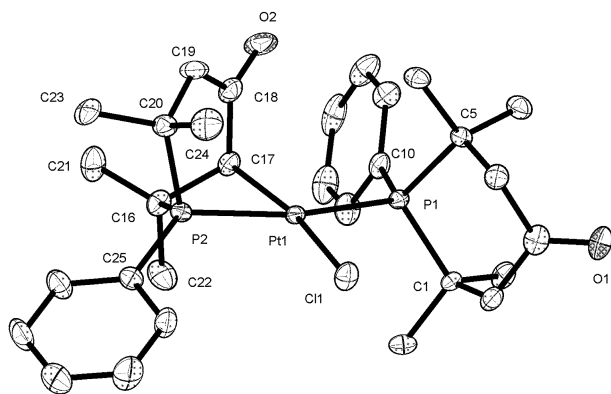


Fig. 5 Crystal structure of complex **3** (50% thermal ellipsoids). All hydrogens have been omitted for clarity.

Table 6 Selected bond distances (Å) and angles (°) for complex **3**

Pt1–C17	2.107(3)	C10–P1–C1	105.67(15)
Pt1–P2	2.2773(10)	C10–P1–C5	108.04(15)
Pt1–P1	2.3251(9)	C1–P1–C5	104.62(15)
Pt1–C11	2.3799(10)	C25–P2–C16	114.48(16)
P1–C10	1.822(3)	C25–P2–C20	109.34(16)
P1–C1	1.881(3)	C16–P2–C20	106.44(16)
P1–C5	1.887(3)	C16–P2–Pt1	87.05(12)
P2–C25	1.813(3)	C17–C16–P2	89.5(2)
P2–C16	1.841(3)	C16–C17–Pt1	101.4(2)
P2–C20	1.846(3)	C17–Pt1–P2–C16	24.34(14)
C17–Pt1–P2	66.20(10)	Pt1–P2–C16–C17	–30.76(17)
C17–Pt1–P1	97.03(10)	P2–C16–C17–Pt1	34.29(17)
P2–Pt1–P1	163.23(3)	P2–Pt1–C17–C16	–29.85(17)
P2–Pt1–C11	100.80(4)		

P(1) adopts a near-perfect mirror symmetric chair conformation with the phenyl substituent almost eclipsing the Pt–C bond.

It is likely that the selective formation of this unprecedented cyclometallated product (presumably *via* **2**) under such mild conditions is associated with the activation of the CH by the α -carbonyl group. The IR spectrum of **3** had $\nu(\text{CO})$ bands at 1705 and 1654 cm^{-1} with the lower frequency band assigned to the CO adjacent to the metallated carbon. The *ca.* 50 cm^{-1} lowering is consistent with delocalisation of the δ^- charge on to the C=O through partial enolate character in the Pt–C–C(O) moiety. However, the crystallographically determined CO bond lengths do not reflect this effect and do not differ significantly. The C–C(O) lengths in the two phosphine ligands in **3** are also

similar (C–O in P(1) ligand 1.218(4) Å, in P(2) ligand 1.221(4) Å; PtC–C(O) in the P(2) ligand is 1.486(5) Å while the two C–C(O) in P(1) ligand are 1.499(5) Å and 1.500(5) Å).

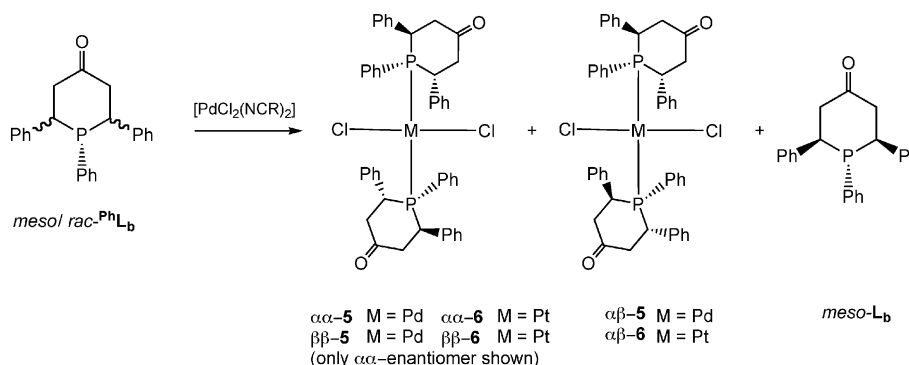
Thus L_b undergoes cycloplatination readily but not cyclopalladation (see above). However, upon refluxing a mixture of **1** and NEt_3 in toluene for 20 h, several products were formed but the major one (*ca.* 70%) had very similar ^{31}P parameters to **3** (δ_{A} 41.1 ppm, δ_{X} –12.7 ppm, $J(\text{P}_{\text{A}}\text{P}_{\text{X}})$ 423 Hz) and is therefore assigned the analogous structure **4**.

Palladium(II) and platinum(II) complexes of $^{\text{Ph}}\text{L}_b$

When a 1 : 2 *meso* : *rac* mixture of isomers of $^{\text{Ph}}\text{L}_b$ (2 equiv.) was added to $[\text{PdCl}_2(\text{NCPh})_2]$ in CH_2Cl_2 , the ^{31}P NMR spectrum of the resulting solution showed no free ligand remained, consistent with complexation of both *meso*- and *rac*- $^{\text{Ph}}\text{L}_b$ to give several species (see Experimental section). Addition of further 1 : 2 *meso* : *rac*- $^{\text{Ph}}\text{L}_b$ led to a great simplification of the spectrum: a singlet for *meso*- $^{\text{Ph}}\text{L}_b$ and two singlets assigned to the $\alpha\alpha/\beta\beta$ - and $\alpha\beta$ -diastereoisomers of **5** (see Scheme 7). Thus palladium(II) has a significant preference for complexing with *rac*- $^{\text{Ph}}\text{L}_b$ over *meso*- $^{\text{Ph}}\text{L}_b$.

Even greater isomer-selective complexation was observed when an excess of *rac*/*meso*- $^{\text{Ph}}\text{L}_b$ was added to $[\text{PtCl}_2(\text{NCBu}^i)_2]$ in toluene and the mixture refluxed for 16 h. The ^{31}P NMR spectrum of the resulting solution showed unreacted *meso*- $^{\text{Ph}}\text{L}_b$ to be present and the yellow solid product had two Pt-containing species in the ratio of *ca.* 1 : 10 (δ 16.3, $^1J(\text{PtP})$ 2700 Hz and δ 20.7, $^1J(\text{PtP})$ 2770 Hz) assigned to the diastereoisomers of *trans*- $[\text{PtCl}_2(\text{rac-}^{\text{Ph}}\text{L}_b)_2]$, $\alpha\beta$ -**6** and $\alpha\alpha/\beta\beta$ -**6**. This reaction is so selective that we have used it as a way of separating *rac*- $^{\text{Ph}}\text{L}_b$ and *meso*- $^{\text{Ph}}\text{L}_b$ by decomplexing *rac*- $^{\text{Ph}}\text{L}_b$ from **6** with KCN (see Experimental section).

The preference of platinum(II) and palladium(II) to complex *rac*- $^{\text{Ph}}\text{L}_b$ over *meso*- $^{\text{Ph}}\text{L}_b$ is consistent with access to the P lone pair in *meso*- $^{\text{Ph}}\text{L}_b$ being inhibited by the *cis*-2,6-phenyl substituents. Further insight into this diastereoisomer preference was gained from a DFT study. Geometry optimisations were carried out for the complexes formed by chair and twist conformations for *meso* (**A** and **B**) and *rac* isomers of $^{\text{Ph}}\text{L}_b$ bound to a $[\text{PtCl}_2]^-$ fragment (with Pt at the lone pair site). Their energies are given in Table 7. Chair and twist conformers did not interconvert during geometry optimisation indicating that they are robust local minima but for *meso*-**A** and *meso*-**B**, the twist conformers distorted to twist-boat conformations upon optimisation.



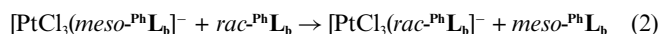
Scheme 7

Table 7 Relative energy and expected distribution of conformers for $[\text{PtCl}_3(\text{P}^{\text{h}}\text{L}_b)]^-$

Isomer	Conformation	Relative $E/\text{kJ mol}^{-1}$
<i>meso-A</i>	eq-chair	0.0
	twist	34.7
<i>meso-B</i>	ax-chair	4.4
	twist	4.6
<i>rac</i>	eq-chair	8.0
	ax-chair	33.3
	twist	3.2

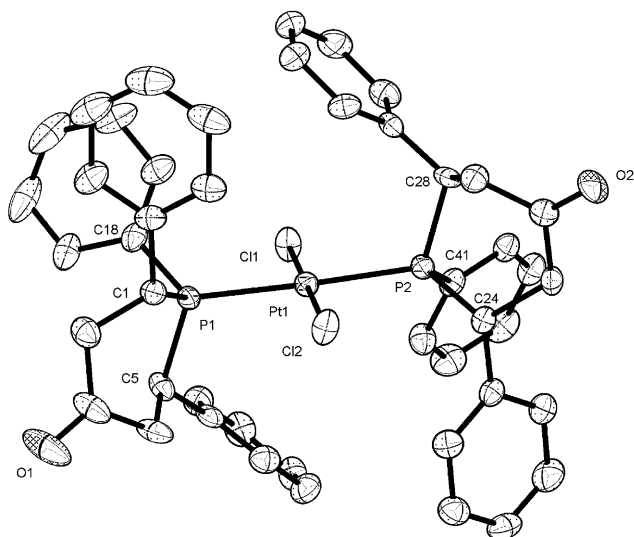
From the data in Table 7 we can make the following observations: (1) Twist and eq-chair conformers of complexed *rac*- $\text{P}^{\text{h}}\text{L}_b$ will be populated at room temperature but the ax-chair conformer (which is accessible in the free ligand) is highly unfavourable. This is presumably due to a steric clash of the metal fragment with the adjacent axial C–Ph substituent; the crystal structure of **6** described below does indeed contain twist conformations of *rac*- $\text{P}^{\text{h}}\text{L}_b$. (2) The preferred conformation (eq-chair) for complexed *meso-A* remains as in the uncoordinated ligand. (3) For complexed *meso-B* (not observed experimentally) the ax-chair and twist conformations will have approximately equal energy.

From the data in Tables 4 and 7, ΔH for the reaction shown in eqn (2) is -7.9 kJ mol^{-1} . This is in qualitative agreement with the experimental observation of the greater coordinating strength of *rac*- $\text{P}^{\text{h}}\text{L}_b$ than *meso*- $\text{P}^{\text{h}}\text{L}_b$.



Notably the data in Tables 4 and 7 indicate that the *meso-B* isomer would displace *rac*- $\text{P}^{\text{h}}\text{L}_b$ from its $[\text{PtCl}_3\text{L}]^-$ complex ($\Delta E -4.6 \text{ kJ mol}^{-1}$), though testing this hypothesis experimentally is precluded because the *meso-B* form of $\text{P}^{\text{h}}\text{L}_b$ was not observed under the conditions we used for the synthesis of $\text{P}^{\text{h}}\text{L}_b$.

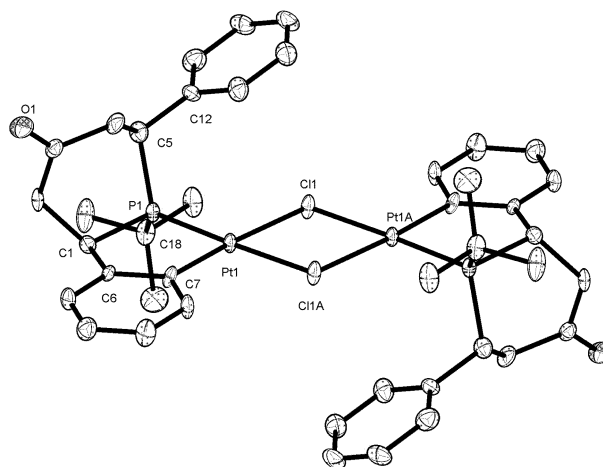
Crystals of $\alpha\alpha/\beta\beta$ -*trans*- $[\text{PtCl}_2(\text{rac}\text{-}\text{P}^{\text{h}}\text{L}_b)_2]$ ($\alpha\alpha/\beta\beta$ -**6**) were grown by slow evaporation of a CDCl_3 solution and the X-ray crystal structure determined (see Fig. 6, Table 8). The structure shown is of the $\alpha\alpha$ -enantiomer although the crystal contains a racemic mixture

**Fig. 6** Crystal structure of complex $\alpha\alpha$ -**6** (50% thermal ellipsoids). All hydrogens have been omitted for clarity.**Table 8** Selected bond distances (Å) and angles ($^\circ$) for complex $\alpha\alpha$ -**6**

Pt1–Cl1	2.2990(12)	P2–C28	1.861(4)
Pt1–P2	2.3078(12)	P2–C24	1.874(4)
Pt1–P1	2.3114(11)	C18–P1–C5	107.5(2)
Pt1–Cl2	2.3245(12)	C18–P1–C1	102.2(2)
P1–C18	1.815(5)	C5–P1–C1	101.87(19)
P1–C5	1.863(4)	C41–P2–C28	107.7(2)
P1–C1	1.870(4)	C41–P2–C24	102.92(19)
P2–C41	1.829(4)	C28–P2–C24	101.87(19)

of the two enantiomers. Each molecule of **6** in the crystal has approximate C_2 symmetry with the platinum coordination *trans* and square planar as expected. The individual ligands adopt twist conformations with the phenyl groups in the 2- and 6-positions in pseudo-equatorial sites and the metal and 1-phenyl group isoclinal. The orientation of the phosphine ligands, as regards rotation about the Pt–P bonds, leaves both the P-phenyl groups close to the same chloride ligand (Cl(1)) and one of the C-phenyl groups on each ligand shielding the axial sites on the platinum centre.

Upon treatment of $[\text{PtCl}_2(\text{NCBu}^1)_2]$ with 1 equivalent of *meso*- $\text{B}^{\text{h}}\text{L}_b$ in refluxing toluene, a precipitate of the binuclear cyclometalated complex **7** forms whose structure was assigned on the basis of NMR spectroscopy and X-ray crystallography (see below). The ^{31}P NMR spectrum of **7** showed a singlet at high frequency (δ 64.9) and a large $^1J(\text{PtP})$ of 4846 Hz, consistent with the five-membered metallacycle **7** containing $\mu\text{-Cl}$ ligands. Crystals of $[\text{Pt}_2(\mu\text{-Cl})_2(\text{meso}\text{-}\text{B}^{\text{h}}\text{L}_b\text{-}2\text{H}_2)]$ (**7**) as a toluene solvate were grown by slow evaporation of a CH_2Cl_2 /toluene solution and the X-ray crystal structure determined (see Fig. 7, Table 9). The molecular structure has exact C_i symmetry with the metal atoms in square planar coordination and the entire central $\text{Pt}_2(\mu\text{-Cl})_2(\text{PCCC})_2$ unit close to planar.

**Fig. 7** Crystal structure of complex **7** (50% thermal ellipsoids). All hydrogens have been omitted for clarity. The symmetry operation invoked for the atoms with 'A' letters is $(1 - x, 2 - y, 1 - z)$.

When a 1 : 1 mixture of *meso* : *rac*- $\text{B}^{\text{h}}\text{L}_b$ was reacted with $[\text{PtCl}_2(\text{NCBu}^1)_2]$ in refluxing toluene, binuclear **7** precipitates from solution as expected and in the filtrate, a single complex was identified by its characteristic AX pattern in the ^{31}P NMR

Table 9 Selected bond distances (Å) and angles (°) for complex **7**

Pt1–C7	2.017(6)	C1–P1–C18	105.4(3)
Pt1–P1	2.1914(18)	C1–P1–C5	101.8(3)
Pt1–C11A	2.3937(17)	C18–P1–C5	109.1(3)
Pt1–C11	2.4315(16)	C1–P1–Pt1	106.6(2)
P1–C1	1.848(6)	C6–C1–P1	107.5(4)
P1–C18	1.858(6)	C6–C7–Pt1	121.7(5)
P1–C5	1.862(7)	C7–C6–C1	119.5(5)
C1–C6	1.511(9)	Pt1–P1–C1–C6	8.5(5)
C7–C6	1.417(9)	P1–Pt1–C7–C6	3.9(5)
C7–Pt1–P1	84.0(2)	Pt1–C7–C6–C1	1.2(8)
C7–Pt1–C11A	95.8(2)	P1–C1–C6–C7	–6.6(7)
P1–Pt1–C11	99.90(6)		

Table 10 Selected bond distances (Å) and angles (°) for complex $\alpha\beta$ -**9**

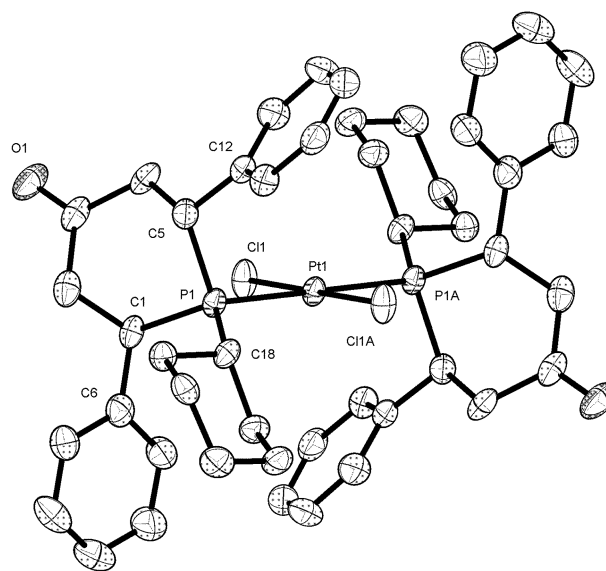
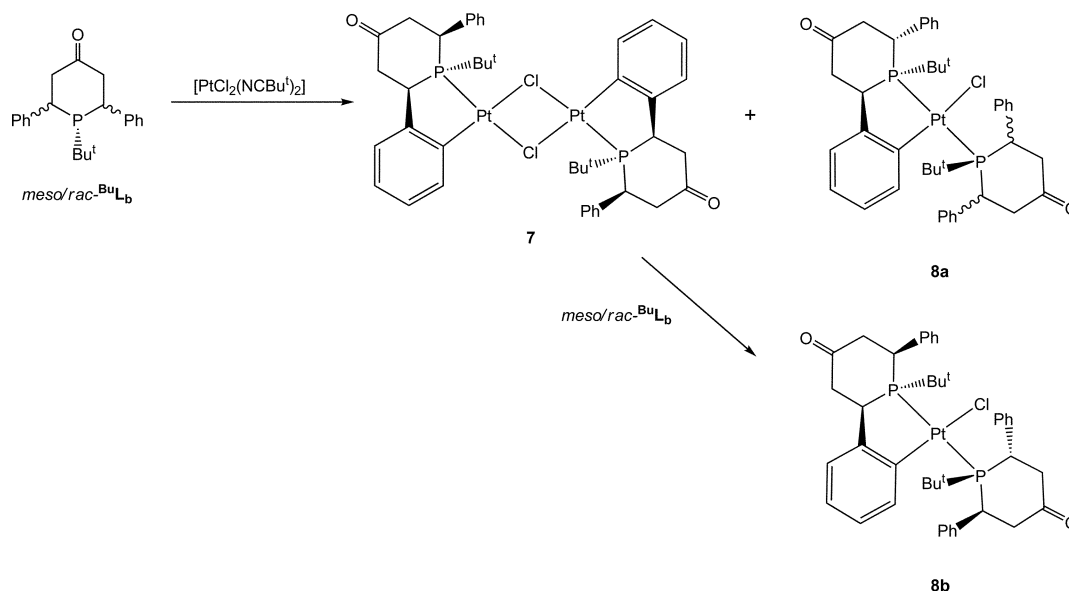
Pt1–C11	2.3169(13)	P1–C1	1.881(5)
Pt1–P1	2.3322(13)	C18–P1–C5	104.9(2)
P1–C18	1.847(5)	C18–P1–C1	110.1(2)
P1–C5	1.873(6)	C5–P1–C1	99.4(2)

spectrum. The data for this species (δ_A 60.0, $^1J(\text{PtP}_A)$ 2994 Hz, δ_X 35.5, $^1J(\text{PtP}_X)$ 2900 Hz, $^2J(\text{P}_A\text{P}_X)$ 396 Hz) are consistent with structure **8a** (see Scheme 8) which features a cyclometallated *rac*- Bu^tL_b . Cyclometallated *rac*- Bu^tL_b rather than *meso*- Bu^tL_b is suggested because isolated **7**: (i) does not react with an excess of pure *meso*- Bu^tL_b and (ii) reacts with *meso/rac*- Bu^tL_b to give a different, bridge-cleaved product according to its ^{31}P NMR data (δ 64.1, $^1J(\text{PtP}_A)$ 3063 Hz, δ 33.6, $^1J(\text{PtP}_A)$ 3016 Hz, $^2J(\text{P}_A\text{P}_X)$ 426 Hz) assigned structure **8b**. The observation of complexes **7** and **8a** establishes that both *meso*- and *rac*- Bu^tL_b undergo orthometallation.

The platinum(II) coordination chemistry of PhL_b and Bu^tL_b differs in that a complex of the type *trans*- $[\text{PtCl}_2(\text{R}\text{L}_b)_2]$ was observed only with PhL_b and cyclometallation was only observed with Bu^tL_b , indicating that the Bu^t substituent promotes the C–H activation. In view of these differences, it was of interest to investigate ligands of intermediate bulk, such as *meso/rac*- CyL_b .

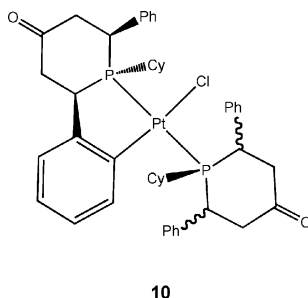
The reaction of 2 equivalents of pure *rac*- CyL_b with $[\text{PtCl}_2(\text{NCBu}^t)_2]$ in refluxing toluene gave two similar species in *ca.* 1 : 1 ratio (δ 17.3, $^1J(\text{PtP}_A)$ 2591 Hz and δ 15.0, $^1J(\text{PtP}_A)$ 2535 Hz) assigned to the diastereoisomers of *trans*- $[\text{PtCl}_2(\text{rac}\text{-}\text{CyL}_b)_2]$, $\alpha\alpha/\beta\beta$ -**9** and $\alpha\beta$ -**9**. In this reaction *rac*- CyL_b is behaving in a similar fashion to *rac*- PhL_b . Crystals of $\alpha\beta$ -**9** were grown from slow evaporation of

its toluene solution and the X-ray crystal structure determined (see Fig. 8, Table 10). Molecules of $\alpha\beta$ -**9** have exact inversion symmetry (confirming the geometric and diastereoisomer assignment). As in all the complexes reported in this paper, one P–C bond of the PC_5 moiety (here P1–C5) is perpendicular to the metal

**Fig. 8** Crystal structure of complex $\alpha\beta$ -**9** (50% thermal ellipsoids). All hydrogens have been omitted for clarity. The symmetry operation invoked for the atoms with 'A' letters is $(1/2 - x, 3/2 - y, 2 - z)$.**Scheme 8**

coordination plane. The ring has a twist conformation with the metal and cyclohexyl groups isoclinial.

The reaction of a mixture of *meso/rac*- CyL_b with $[\text{PtCl}_2(\text{NCBu}^t)_2]$ in refluxing toluene gave the expected $\alpha\alpha/\beta\beta$ -**9** and $\alpha\beta$ -**9** along with a third species whose characteristic AX pattern (δ_A 51.8, $^1J(\text{PtP}_A)$ 2892 Hz, δ_X 29.4, $^1J(\text{PtP}_X)$ 2938 Hz, $J(\text{P}_A\text{P}_X)$ 403 Hz) indicated that *meso*- CyL_b had cyclometallated to give a complex tentatively assigned the structure **10**, i.e. an analogue of **8b**.



10

The studies with *meso*- and *rac*- CyL_b support the conclusion that the *meso*-isomer is more susceptible than the *rac*-isomer to cyclometallation and that a bulky P–R substituent promotes this reaction.

Conclusion

The palladium(II) and platinum(II) coordination chemistry of the bulky phosphorinanones PhL_a , PhL_b , BuL_b and CyL_b has revealed that the combination of the six-membered phosphacycle, the ketone function and the exocyclic phenyl groups gives these ligands unusual properties. For example, cyclometallation of PhL_a occurs at the activated carbon adjacent to the carbonyl to form a remarkable bicyclic complex whereas cyclometallation of BuL_b occurs on the exocyclic phenyl substituent. Unexpectedly, there is such a degree of discrimination in favour of complexation of the less stable *rac*- PhL_b over the *meso*- PhL_b that this has been exploited in a method for the separation of the isomers. DFT calculations suggest that the source of the greater ligating power of *rac*- R^bL_b can be traced to ring conformational effects: the twist conformation which is accessible in the free *rac*- R^bL_b becomes favoured upon metal binding because the R and metal groups occupy synclinal sites and thereby minimise steric clashing. In other words, *rac*- R^bL_b is better preorganised for complexation than *meso*- R^bL_b .

Experimental

Unless otherwise stated, all work was carried out under a dry nitrogen atmosphere, using standard Schlenk line techniques. Dry N_2 -saturated solvents were collected from a Grubbs system¹¹ in flame and vacuum dried glassware. ^1H , ^{13}C and ^{31}P NMR spectra were recorded at 400, 100, and 121 MHz respectively at +23 °C. Mass spectra were recorded on a VG Analytical Autospec (EI) or VG Analytical Quattro (ESI). Elemental analyses were carried out by the Microanalytical Laboratory of the School of Chemistry, University of Bristol. IR spectra were recorded on a Perkin Elmer 1600 Series Spectrometer in dichloromethane. $[\text{PtCl}_2(1,5\text{-cod})]$,¹² $[\text{PdCl}_2(\text{NCPH})]$ ¹³ and $[\text{PtCl}_2(\text{NCBu}^t)_2]$ ¹⁴ starting materials

were made by literature methods. All other starting materials were purchased from Aldrich or Strem.

Preparation of 2,2,6,6-tetramethyl-1-phenyl-4-phosphorinanone (L_a)

A 250 cm^3 , 2-necked, round-bottomed flask was charged with phorone (2,6-dimethyl-2,5-heptadien-4-one) (7.82 g, 57.0 mmol). Phenylphosphine (5.00 cm^3 , 5.00 g, 45.4 mmol) was added to the flask and the mixture was refluxed at 120 °C for 21 h. Upon cooling the flask, a yellow waxy solid was obtained. This was triturated with pentane (2 \times 30 cm^3) to give a white solid (6.53 g, 58%). $^{31}\text{P}\{^1\text{H}\}$ NMR (CDCl_3): δ = 17.1 (s). ^1H NMR (CDCl_3): δ = 7.36–7.19 (5H, m, ArH), 2.90 (2H, d, $^2J(\text{HH})$ 13 Hz, CH_2), 2.32 (2H, dd, $^2J(\text{HH})$ 13 Hz $^3J(\text{PH})$ 5 Hz, CH_2), 1.32 (6H, d, $^3J(\text{PH})$ 8 Hz, CH_3), 0.93 (6H, d, $^3J(\text{PH})$ 11 Hz, CH_3). ^{13}C NMR (CDCl_3): δ = 211.4 (s, CO), 135.8 (d, $^2J(\text{PC})$ 23 Hz), 129.7 (s), 128.4 (d, $^3J(\text{PC})$ 9 Hz), 53.1 (d, $^3J(\text{PC})$ 2 Hz, CH_2), 35.2 (d, $^1J(\text{PC})$ 18 Hz, $\text{C}(\text{CH}_3)_2$), 31.1 (d, $^2J(\text{PC})$ 31 Hz, CH_3), 30.0 (d, $^2J(\text{PC})$ 11 Hz, CH_3). m/z (EI) 248 (M^+). Elemental analysis (calc) C: 72.60 (71.98), H: 8.50 (8.42%). IR (CH_2Cl_2): ν_{CO} 1701.2 cm^{-1} .

Preparation of 1,2,6-triphenyl-4-phosphorinanone (PhL_b)

In a 100 cm^3 , 2-necked, round-bottomed flask, dibenzylideneacetone (3.19 g, 13.6 mmol) was dissolved in acetonitrile (20 cm^3) and phenylphosphine (1.50 g, 13.6 mmol) was added to the solution. *para*-Toluenesulfonic acid (0.50 g, 1.36 mmol) was added to the flask and the yellow solution refluxed at 105 °C for 48 h. A creamy-white solid which precipitated from the orange solution was washed with diethyl ether and crystallised from a saturated acetonitrile solution to give the product as a white solid (1.97 g, 42%). The product was a 1 : 3 *meso* : *rac* mixture of isomers. $^{31}\text{P}\{^1\text{H}\}$ NMR (CDCl_3): δ = –2.2 (s, *meso*), –5.6 (s, *rac*). ^1H NMR (CDCl_3): δ = 7.40–7.00 (13H, m, Ar), 6.82–6.68 (2H, m, Ar), 3.90–3.65 (2H, m, CH), 3.20–2.80 (4H, m, CH_2). m/z (EI) 344 (M^+). Elemental analysis (calc) C: 79.55 (80.21) H: 6.57 (6.15%).

Preparation of 1-cyclohexyl-2,6-diphenyl-4-phosphorinanone (CyL_b)

Preparation of 4 : 1 *meso* : *rac*- CyL_b . In a 100 cm^3 , 2-necked, round-bottomed flask, dibenzylideneacetone (2.343 g, 10.2 mmol) was dissolved in acetonitrile (20 cm^3) and cyclohexylphosphine (1.162 g, 10.0 mmol) was added to the solution. *para*-Toluenesulfonic acid (0.475 g, 2.5 mmol) was added to the flask and the yellow solution refluxed for 144 h. A creamy-white solid which precipitated from the orange solution was washed with diethyl ether and crystallised from a saturated acetonitrile solution to give the product as a white solid (1.330 g, 38%). The product was a 4 : 1 *meso* : *rac* mixture of isomers. $^{31}\text{P}\{^1\text{H}\}$ NMR (toluene): δ = 6.2 (s, *meso*), 0.9 (s, *rac*). ^1H NMR (CDCl_3): δ = 7.39–7.13 (10H, m, Ar), 3.67–3.46 (2H, m, CH), 3.20–2.93 (2 H, m, CH_2), 2.92–2.75 (2 H, m, CH_2), 1.78–1.31 (11H, m, Cy–H). ^{13}C NMR (CDCl_3): δ = 208.2 (s, CO), 126.8–141.7 (12 C, m, Ar), 49.5 (d, $^2J(\text{PC})$ 13 Hz, CH_2), 40.1 (d, $^1J(\text{PC})$ 15 Hz, CH), 32.4 (d, $^1J(\text{PC})$ 19 Hz, $\text{CH}(\text{Cy})$), 28.9 (d, $^3J(\text{PC})$ 8 Hz, CH_2), 27.5 (d, $^2J(\text{PC})$ 9 Hz, CH_2), 26.1 (s, CH_2). m/z (EI) 350 (M^+). HRMS (EI): Calculated for $\text{C}_{23}\text{H}_{27}\text{OP}$: 350.1800. Found 350.1802.

Preparation of 1 : 4 meso : rac-^{Cy}L_b. A 100 cm³, 2-necked, round-bottomed flask was charged with dibenzylideneacetone (4.713 g, 20.5 mmol). Cyclohexylphosphine (2.323 g, 20.0 mmol) was added to the flask and the mixture was refluxed at 120 °C for 36 h. When the mixture cooled to ambient temperature, a yellow oil was observed which was triturated with acetonitrile (2 × 3 cm³) to give the product as a creamy-white solid (2.651 g, 38%). The product was a 1 : 4 *meso* : *rac* mixture of isomers. From this mixture pure *rac*-^{Cy}L_b was recrystallised from acetonitrile. ³¹P{¹H} NMR (CDCl₃): δ = 0.9 (s, *rac*).

Preparation of 1-*tert*-butyl-2,6-diphenyl-4-phosphorinanone (^{Bu}L_b)

Preparation of pure *meso*-^{Bu}L_b. In a 100 cm³, 2-necked, round-bottomed flask dibenzylideneacetone (2.34 g, 10.0 mmol) was dissolved in acetonitrile (20 cm³) and *tert*-butylphosphine (0.82 g, 9.07 mmol) was added to the solution. *para*-Toluenesulfonic acid (0.50 g, 2.60 mmol) was added to the flask and the yellow solution refluxed at 105 °C for 72 h. On cooling the mixture, a lemon solid precipitated from the dark orange solution. The solid was filtered off and washed with cold acetonitrile (10 cm³) to give a yellow solid (1.56 g, 53%). ³¹P{¹H} NMR (CDCl₃): δ = 17.9 (s). ¹H NMR (CDCl₃): δ = 7.45–7.10 (10H, m, Ar), 3.33–3.14 (2H, m, CH), 2.92 (2H, td, *J*(HH) 14 Hz, *J*(HH) 7 Hz, CH₂), 2.79–2.57 (2H, m, CH₂), 0.64 (9H, d, ²*J*(PC) 11 Hz, CH₃). ¹³C NMR (CDCl₃): δ = 208.3 (s, CO), 143.7 (d, ²*J*(PC) 9 Hz, *ipso*-C), 128.9 (s), 128.3 (d, ³*J*(PC) 9 Hz), 126.8 (s), 50.2 (d, ²*J*(PC) 11 Hz, CH₂), 40.8 (d, ¹*J*(PC) 20 Hz, CHPh), 30.6 (d, ¹*J*(PC) 20 Hz, C(CH₃)₃), 28.4 (d, ²*J*(PC) 11 Hz, CH₃). *m/z* (EI) 324 (M⁺). Elemental analysis (calc) C: 77.92 (77.75) H: 8.21 (7.77%).

Preparation of 1 : 1 *meso* : *rac*-^{Bu}L_b. A 50 cm³, 2-necked, round-bottomed flask was charged with dibenzylideneacetone (2.34 g, 10.0 mmol). *tert*-Butylphosphine (0.82 g, 9.07 mmol) was added to the flask and the mixture was heated at 120 °C for 72 h. Upon cooling the flask, an off-white, glassy solid was obtained. This was triturated with pentane (2 × 30 cm³) to give an off-white solid (2.79 g, 95%). ³¹P{¹H} NMR (CDCl₃): δ = 17.9 (s, *meso*), 17.0 (s, *rac*).

Preparation of *trans*-[PdCl₂(L_a)₂] (1)

Ligand L_a (0.27 g, 1.08 mmol) was dissolved in toluene (4 cm³) and [PdCl₂(NCPPh)₂] (0.20 g, 0.52 mmol) was added. A yellow suspension formed rapidly. The solvent was removed *in vacuo* to give a yellow solid (1) (0.34 g, 97%). ³¹P{¹H} NMR (CDCl₃): δ = 42.2 (s). ¹H NMR (CDCl₃): δ = 7.97–7.89 (4H, m, Ar), 7.48–7.38 (6H, m, Ar), 3.40 (4H, dt, ²*J*(HH) 15 Hz, *J*(PC) 5 Hz, CH₂), 2.44 (4H, dt, ²*J*(HH) 15 Hz, *J*(PC) 9 Hz, CH₂), 1.86 (12H, t, *J*(PC) 9 Hz, CH₃), 1.24 (12 H, t, *J*(PC) 6 Hz, CH₃). ¹³C NMR (CDCl₃): δ = 135.1 (s), 130.3 (s), 127.5 (s), 55.3 (s, CH₂), 38.3 (t, *J*(PC) 8 Hz, P–C), 31.7 (t, *J*(PC) 10 Hz, CH₃), 29.4 (s, CH₃). *m/z* (ESI) 638 (M⁺ – Cl). IR (CH₂Cl₂): ν_{CO} 1705.9 cm⁻¹. Elemental analysis (calc) C: 54.02 (53.50) H: 6.22 (6.30%).

Preparation of *trans*-[PtCl₂(L_a–3H)(L_a)] (3)

Ligand L_a (0.280 g, 1.13 mmol) was dissolved in CH₂Cl₂ (4 cm³), [PtCl₂(cod)] (0.184 g, 0.48 mmol) was added and the mixture refluxed for 4 d. The solvent was then removed *in vacuo* and

the white solid obtained redissolved in CH₂Cl₂. Crystalline 3 was obtained by slow diffusion of hexane into this CH₂Cl₂ solution (0.130 g, 32%). ³¹P{¹H} NMR (CDCl₃): δ = 38.2 (d, ²*J*(PP) 407 Hz, ¹*J*(PtP) 2948 Hz), –13.0 ppm (d, ²*J*(PP) 407 Hz, ¹*J*(PtP) 2225 Hz). ¹H NMR (CDCl₃): δ = 8.10–7.36 (10H, m, Ar), 4.08 (1H, dd, *J*(HH) 3 Hz, ³*J*(PC) 17 Hz, CH), 3.79 (1H, dd, ²*J*(HH) 7 Hz, ³*J*(PC) 20 Hz, CH), 2.83 (1H, dd, ²*J*(HH) 8 Hz, ³*J*(PC) 27 Hz, CH), 2.33 (1H, dd, ²*J*(HH) 11 Hz, ³*J*(PC) 19 Hz, CH), 2.22 (1H, dd, ²*J*(HH) 12 Hz, ³*J*(PC) 30 Hz, CH), 2.19 (1H, d, ³*J*(PC) 20 Hz, CH), 2.07–1.96 (1H, m, PtCH), 1.84 (3H, d, ³*J*(PC) 16 Hz, CH₃), 1.65 (3H, d, ³*J*(PC) 18 Hz, CH₃), 1.54 (3H, d, ³*J*(PC) 18 Hz, CH₃), 1.38 (3H, d, ³*J*(PC) 9 Hz, CH₃), 1.20 (3H, d, ³*J*(PC) 13 Hz, CH₃), 1.10 (3H, d, ³*J*(PC) 12 Hz, CH₃). ¹³C NMR (CDCl₃): δ = 209.4 (d, ³*J*(PC) 4.6 Hz, CO), 203.5 (d, ³*J*(PC) 14 Hz, CO), 135.8 (d, ¹*J*(PC) 22 Hz, *ipso*-C), 135.1 (dd, ²*J*(PC) 8 Hz, ⁴*J*(PC) 3 Hz), 133.4 (d, ²*J*(PC) 8 Hz), 132.0 (d, ²*J*(PC) 2 Hz), 130.0 (d, ²*J*(PC) 2 Hz), 128.9 (d, ²*J*(PC) 10 Hz), 127.9 (d, ²*J*(PC) 9 Hz), 124.5 (dd, ²*J*(PC) 36 Hz, ⁴*J*(PC) 11 Hz, *ipso*-C), 56.4 (s, CH₂), 55.4 (s, CH₂), 53.2 (d, ²*J*(PC) 2 Hz, CH₂), 43.6 (d, ¹*J*(PC) 30 Hz, C(CH₃)₃), 40.0 (dd, ¹*J*(PC) 19 Hz, ³*J*(PC) 4 Hz, C(CH₃)₃), 38.5 (dd, ¹*J*(PC) 19 Hz, ³*J*(PC) 2 Hz, C(CH₃)₃), 37.3 (d, ¹*J*(PC) 29 Hz, C(CH₃)₃), 32.5 (s, CH₃), 32.4 (d, ²*J*(PC) 3 Hz, CH₃), 31.6 (d, ²*J*(PC) 7 Hz, CH₃), 30.6 (d, ²*J*(PC) 5 Hz, CH₃), 28.9–28.7 (m, CH₃), 26.7 (t, *J*(PC) 4 Hz, CH₃), 26.4 (t, *J*(PC) 3 Hz, CH₃). The cyclometallated carbon has not been identified. *m/z* (EI) 726 (M⁺), 689 (M⁺ – Cl). IR (CH₂Cl₂): ν_{CO} 1704.5 cm⁻¹, 1654.3 cm⁻¹.

Preparation of *trans*-[PdCl₂(*rac*-^{Ph}L_b)₂] (5)

A 1 : 2 mixture of *meso* : *rac*-^{Ph}L_b (0.10 g, 0.30 mmol) was dissolved in toluene (10 cm³), [PdCl₂(NCPPh)₂] (0.06 g, 0.15 mmol) was added and the solution was refluxed at 120 °C for 6 h during which time a pale yellow solid precipitated from the solution. The solid was filtered off and washed with toluene to give the product as a pale yellow powder (0.06 g, 69% based on *rac*-isomer). ³¹P{¹H} NMR (CDCl₃): δ = 28.4 (s) which indicates that only one of the diastereoisomers had precipitated tentatively assigned to *αα*/*ββ*-5 by analogy with the platinum species *αα*/*ββ*-6. ¹H NMR (CDCl₃): δ = 7.24–6.82 (30, m, Ar), 5.20 (2H, dd, ²*J*(PC) 17 Hz, ²*J*(HH) 2 Hz, CH), 4.20 (2H, dd, ²*J*(PC) 18 Hz, ²*J*(HH) 3 Hz, CH), 4.10–3.99 (2H, m, CH₂), 3.19–2.99 (4H, m, CH₂), 2.84–2.68 (2H, m, CH₂). *m/z* (EI) 865 (M⁺).

Reaction of *meso* : *rac*-^{Ph}L_b with [PdCl₂(NCPPh)₂]

A 1 : 2 mixture of *meso* : *rac*-^{Ph}L_b (0.028 g, 0.08 mmol) was dissolved in CH₂Cl₂ in an NMR tube at room temperature and [PdCl₂(NCPPh)₂] (15 mg, 0.04 mmol) was added. The ³¹P NMR spectrum of the resulting solution changed with time. The initial spectra showed the presence of 2 species in addition to *αα*/*ββ*-5: an AB pattern (δ_A 28.7, δ_B 21.7, ²*J*_{AB} 434 Hz) assigned to *trans*-[PdCl₂(*rac*-^{Ph}L_b)(*meso*-^{Ph}L_b)] and a singlet (δ 22.4) assigned to *αβ*-5 or *trans*-[PdCl₂(*meso*-^{Ph}L_b)₂]. The proportions of products changed over 3 days and the final spectrum showed the presence of mainly *αα*/*ββ*-5.

Preparation of *trans*-[PtCl₂(*rac*-^{Ph}L_b)₂] (6)

A 1 : 2 mixture of *meso* : *rac*-^{Ph}L_b (0.34 g, 0.97 mmol) was dissolved in toluene (10 cm³), [PtCl₂(NCBu^t)₂] (0.21 g, 0.49 mmol) was added

and the solution was refluxed at 118 °C for 16 h. A yellow solid precipitated from the solution which was filtered off and washed with toluene (0.13 g, 43% based on *rac*-isomer). $^{31}\text{P}\{^1\text{H}\}$ NMR (CDCl_3): $\delta = 21.27$ (s, $^1J(\text{PtP})$ 2770 Hz, $\alpha\alpha/\beta\beta$ -6), 16.20 (s, $^1J(\text{PtP})$ 2700 Hz, $\alpha\beta$ -6). ^1H NMR (CDCl_3): $\delta = 7.42$ – 6.79 (30, m, Ar), 5.80–5.46 (2H, m, CH), 4.67–4.33 (2H, m, CH), 4.12–3.85 (2H, m, CH_2), 3.34–2.98 (4H, m, CH_2), 2.92–2.69 (2H, m, CH_2). m/z (FAB) 978 ($\text{M}^+ + \text{Na}$).

Separation of *rac*- and *meso*- $\text{P}^{\text{h}}\text{L}_b$ by selective complexation

$[\text{PtCl}_2(\text{rac}-\text{P}^{\text{h}}\text{L}_b)_2]$ (**6**) (0.10 g, 0.11 mmol) was suspended in a mixture of CH_2Cl_2 (5 cm^3) and acetone (5 cm^3). Aqueous KCN solution (3.21 cm^3 , 0.5 M, 1.60 mmol) was added and the mixture then vigorously stirred overnight to produce an emulsion. All the solvents were removed *in vacuo* and to the resulting solid dichloromethane (25 cm^3) and water (10 cm^3) were added. The dichloromethane layer was syringed off and the aqueous layer was washed with dichloromethane ($2 \times 5 \text{ cm}^3$). The combined organic layers were dried over MgSO_4 , filtered and the solvent was removed *in vacuo* to give *rac*- $\text{P}^{\text{h}}\text{L}_b$ as a white solid (0.015 g, 40%). $^{31}\text{P}\{^1\text{H}\}$ NMR (CDCl_3): $\delta = -5.6$ (s).

Preparation of *trans*- $[\text{Pt}_2(\mu\text{-Cl})_2(\text{meso}-\text{B}^{\text{u}}\text{L}_b-2'\text{H})_2]$ (**7**)

meso- $\text{B}^{\text{u}}\text{L}_b$ (0.11 g, 0.34 mmol) was dissolved in toluene (10 cm^3), $[\text{PtCl}_2(\text{NCBu}^{\text{t}})_2]$ (0.15 g, 0.34 mmol) was added and the yellow solution refluxed for 72 h. The product was obtained as a mustard solid, which precipitated from the yellow toluene solution. The product was filtered off and washed with toluene (4 cm^3) (0.17 g, 46%). $^{31}\text{P}\{^1\text{H}\}$ NMR (CDCl_3): $\delta = 64.90$ (s, $^1J(\text{PtP})$ 4846 Hz). ^1H NMR (CDCl_3): $\delta = 8.04$ – 6.86 (18 H, m, Ar), 3.86–3.67 (4H, m), 3.20–2.90 (4H, m), 2.79–2.32 (4H, m), 1.55–1.34 (18H, m, CH_3). ^{13}C NMR (CDCl_3): $\delta = 206.6$ (s, CO), 149.0 (d, $J(\text{HH})$ 13 Hz, Ar), 137.4 (m, Ar), 135.9 (d, $J(\text{HH})$ 18 Hz, Ar), 130.5 (m, Ar), 128.8–128.2 (m, Ar), 127.8 (s, Ar), 127.4 (s, Ar), 126.0 (d, $J(\text{HH})$ 8 Hz, Ar), 125.4 (d, $J(\text{HH})$ 8 Hz, Ar), 123.5 (dd, $J(\text{HH})$ 19 Hz, J 4 Hz, Ar), 45.1 (s), 42.5 (dd, $J(\text{HH})$ 15 Hz, $J(\text{HH})$ 5 Hz), 39.0 (dd, $J(\text{HH})$ 45 Hz, $J(\text{HH})$ 11 Hz), 35.3–34.5 (m), 27.4 (s). m/z (FAB) 1108 (M^+). Elemental analysis (calc) C: 46.6 (45.53) H: 4.95 (4.37%).

Preparation of *trans*- $[\text{PtCl}_2(\text{rac}-\text{C}^{\text{y}}\text{L}_b)_2]$ (**9**)

rac- $\text{C}^{\text{y}}\text{L}_b$ (0.104 g, 0.29 mmol) was dissolved in toluene (10 cm^3), $[\text{PtCl}_2(\text{NCBu}^{\text{t}})_2]$ (0.058 g, 0.13 mmol) was added and the yellow solution refluxed for 24 h. The solvent was then removed *in vacuo* to give the pale yellow solid product. $^{31}\text{P}\{^1\text{H}\}$ NMR (toluene): $\delta = 17.3$ (s, $^1J(\text{PtP})$ 2591 Hz), 15.0 (s, $^1J(\text{PtP})$ 2535 Hz). m/z (EI) 989 $[\text{M} + \text{Na}]^+$.

Computational details

Density functional theory geometry optimisations were calculated for isolated molecules in the gas phase using the Jaguar 6.0¹⁵ suite of programmes, using the standard Becke–Perdew (BP86) functional and the 6-31G* basis set on all atoms except platinum, for which the standard Los Alamos ECP (LACV3P*) basis set was employed.

Table 11 Crystallographic data

Compound	L_a	<i>rac</i> - $\text{C}^{\text{y}}\text{L}_b(\text{O})$	<i>meso</i> - $\text{B}^{\text{u}}\text{L}_b$	1	3	6	7-toluene	$\alpha\beta$ -9
Colour, habit	Colourless block	Colourless plate	Colourless plate	Orange cuboid	Colourless prism	Colourless prism	Colourless plate	Colourless block
Size/mm	$0.2 \times 0.1 \times 0.05$	$0.32 \times 0.08 \times 0.01$	$0.4 \times 0.3 \times 0.3$	$0.48 \times 0.34 \times 0.2$	$0.16 \times 0.16 \times 0.12$	$0.2 \times 0.14 \times 0.06$	$0.3 \times 0.2 \times 0.14$	$0.1 \times 0.1 \times 0.05$
Formula	$\text{C}_{13}\text{H}_{21}\text{OP}$	$\text{C}_{23}\text{H}_{27}\text{O}_2\text{P}$	$\text{C}_{21}\text{H}_{25}\text{OP}$	$\text{C}_{30}\text{H}_{42}\text{Cl}_2\text{O}_2\text{P}_2\text{Pd}$	$\text{C}_{30}\text{H}_{41}\text{ClO}_2\text{P}_2\text{Pt}$	$\text{C}_{46}\text{H}_{42}\text{Cl}_2\text{O}_2\text{P}_2\text{Pt}$	$\text{C}_{49}\text{H}_{56}\text{Cl}_2\text{O}_2\text{P}_2\text{Pt}_2$	$\text{C}_{46}\text{H}_{54}\text{Cl}_2\text{O}_2\text{P}_2\text{Pt}$
<i>M</i>	248.29	366.42	324.38	673.88	726.11	954.73	1199.96	966.82
Crystal system	Monoclinic	Monoclinic	Monoclinic	Monoclinic	Monoclinic	Triclinic	Monoclinic	Monoclinic
Space group	$P2_1/n$	$P2_1/c$	$P2_1/c$	$P2_1/n$	$P2_1/n$	$P1$	$P2_1/c$	$C2/c$
<i>a</i> /Å	7.7616(16)	6.2849(13)	6.0489(18)	8.3599(15)	14.309(3)	10.479(3)	15.415(3)	17.938(4)
<i>b</i> /Å	23.360(5)	22.074(4)	22.056(70)	14.735(3)	14.435(3)	14.369(4)	8.1738(16)	13.963(3)
<i>c</i> /Å	8.1907(16)	14.046(3)	13.959(4)	12.580(2)	15.693(93)	14.537(4)	18.349(4)	16.316(3)
$\alpha/^\circ$	90.00	90.00	90.00	90.00	90.00	116.004(4)	90.00	90.00
$\beta/^\circ$	106.68(3)	102.72(3)	98.366(6)	96.482(4)	113.99(3)	92.782(4)	112.08(3)	65.08(3)
$\gamma/^\circ$	90.00	90.00	90.00	90.00	90.00	95.772(4)	90.00	90.00
<i>V</i> /Å ³	1422.6(6)	1900.8(7)	1842.5(9)	1539.8(5)	2961.3(12)	1946.8(9)	2142.3(9)	4070.6(14)
<i>Z</i>	4	4	4	2	4	2	2	4
μ/mm^{-1}	0.177	1.383	0.152	0.906	4.962	3.862	6.073	8.688
Reflections: total/independent/ R_{int}	15053/3261/0.0304	10169/3068/0.1763	11202/4203/0.0928	9856/3505/0.0346	20860/6809/0.0358	20645/8866/0.0527	14888/4908/0.0603	15450/3784/0.0658
Final <i>R</i>	0.0351	0.0828	0.0679	0.0283	0.0262	0.0366	0.0398	0.03747
Largest peak, hole/ $e \text{ \AA}^{-3}$	0.306, −0.179	0.589, −0.554	0.326, −0.298	0.493, −0.440	1.422, −0.878	1.295, −1.005	3.038, −1.563	1.068, −0.897

Crystal structure determinations

An X-Ray diffraction experiment on **3** was carried out at 100 K on a Bruker SMART APEX diffractometer; experiments on *meso*-^{Ba}**L**_b, **L**_a, **1**, $\alpha\alpha$ -**6** and **7** (as its toluene solvate) were carried out at 173 K on a Bruker SMART diffractometer, using Mo-K α X-radiation ($\lambda = 0.71073 \text{ \AA}$); and experiments on the oxide of *rac*-^{Cs}**L**_b and $\alpha\beta$ -**9** were carried out at 100 K on a Bruker PROTEUM diffractometer using Cu-K α X-radiation ($\lambda = 1.54178 \text{ \AA}$); all data collections were performed using a CCD area-detector, from a single crystal coated in paraffin oil mounted on a glass fibre. Intensities were integrated¹⁶ from several series of exposures, each exposure covering 0.3° in ω . Absorption corrections were based on equivalent reflections using SADABS V2.10,¹⁷ and structures were refined against all F_o^2 data with hydrogen atoms riding in calculated positions using SHELXTL.¹⁸ Crystal and refinement data are given in Table 11.

For **7**, the structure contains a solvent molecule of toluene disordered over two positions for every complex molecule present. The geometry of the toluene was constrained to an ideal geometry and the atoms were refined isotropically. No disorder was present in the other crystal structures and refinements proceeded smoothly to give the structures shown.

CCDC reference numbers 609145–609151 and 611214.

For crystallographic data in CIF or other electronic format see DOI: 10.1039/b607490a

References

1 R. P. Welcher and N. E. Day, *J. Org. Chem.*, 1962, **27**, 1824.

- 2 J. B. Rampal, G. D. Macdonell, J. P. Edasery, K. D. Berlin, A. Rahman, D. van der Helm and K. M. Pietrusiewicz, *J. Org. Chem.*, 1981, **46**, 1156.
- 3 (a) J. B. Rampal, K. D. Berlin, J. P. Edasery, N. Satyamurthy and D. van der Helm, *J. Org. Chem.*, 1981, **46**, 1166; (b) J. B. Rampal, N. Satyamurthy, J. M. Bowen, N. Purdie and K. D. Berlin, *J. Am. Chem. Soc.*, 1981, **103**, 7602.
- 4 (a) M. Slany, M. Schäfer and M. Röper (BASF), *Ger. Pat.*, DE10106348, 2002; (b) G. Eastham (Lucite International), *World Patent*, WO024322, 2004.
- 5 T. Brenstrum, J. Clattenburg, J. Britten, S. Zavorine, J. Dyck, A. J. Robertson, J. McNulty and A. Capretta, *Org. Lett.*, 2006, **8**, 103.
- 6 S. L. Featherman and L. D. Quin, *J. Am. Chem. Soc.*, 1975, **97**, 4349.
- 7 L. A. Paquette, *Angew. Chem., Int. Ed. Engl.*, 1990, **29**, 609.
- 8 J. Weiser, O. Golan, L. Fitjer and S. E. Biali, *J. Org. Chem.*, 1996, **61**, 8277.
- 9 H. Werner and H. J. Kraus, *J. Organomet. Chem.*, 1981, **204**, 415.
- 10 (a) A. J. Cheney, B. E. Mann, B. L. Shaw and R. M. Slade, *J. Chem. Soc. D*, 1970, 1176; (b) A. J. Cheney, B. E. Mann, B. L. Shaw and R. M. Slade, *J. Chem. Soc. A*, 1971, 3833.
- 11 A. B. Pangborn, M. A. Giardello, R. H. Grubbs, R. K. Rosen and F. J. Timmers, *Organometallics*, 1996, **15**, 1518.
- 12 J. X. McDermott, J. F. White and G. M. Whitesides, *J. Am. Chem. Soc.*, 1976, **98**, 6521.
- 13 R. Doyle, P. E. Slade and H. B. Jonassen, *Inorg. Synth.*, 1960, **6**, 218.
- 14 D. Fraccarollo, R. Bertani, M. Mozzon, U. Belluco and R. Michelin, *Inorg. Chim. Acta*, 1992, **201**, 15.
- 15 *Jaguar 6.0*, Schrodinger, LLC, Portland, Oregon, 2005.
- 16 *SAINTE integration software*, Siemens Analytical X-ray Instruments Inc., Madison, WI, 1994.
- 17 G. M. Sheldrick, *SADABS V2.10*, University of Göttingen, Germany, 2003.
- 18 *SHELXTL program system version 5.1*, Bruker Analytical X-ray Instruments Inc., Madison, WI, 1998.